Mausam, (1982), **33**, 3, 343-350

551.553.21 : 551.515.1

Behaviour of monsoon depressions in simple quasi-geostrophic models

SURANJANA SAHA
School of Environmental Sciences, Jawaharlal Nehru University, New Delhi
(Received 27 July 1981)

सार – एकल स्तर भूविक्षेपी कल्प दाबघनत्वी प्रतिदर्श और एक द्विस्तरी भूविक्षेपी – कल्प दाब प्रवणित प्रतिदर्श को मानसून के प्रवाह के व्यवहार के अध्ययन के लिए समाकलित किया गया है। उपयोग में आए आंकड़े ग्रीष्म मानसून प्रयोग (मानेक्स–79) के दौरान के संग्रहित आंकड़े हैं। मानसून अवदावों का गमन का मानसून के प्रवाह का एक प्रमुख अभिलक्षण है, विशेषत: इन प्रतिदर्शों के द्वारा अध्ययन किया गया है। दोनों प्रतिदर्शों के तुलनात्मक कार्य का परीक्षण भी किया गया है।

ABSTRACT. A single level quasi-geostrophic barotropic model and a two level quasi-geostrophic baroclinic model have been integrated to study the behaviour of monsoonal flow. The data utilised are those collected during the summer Monsoon Experiment (Monex-79). The movement of monsoon depressions, an important feature of monsoonal flow, is studied in particular by these models. The comparative performance of the models is also examined.

1. Introduction

The quasi-geostrophic models are known to be not very adequate for predicting the detailed behaviour of atmospheric motion in the low latitudes. However, Shukla and Saha (1970), Mukherji and Datta (1973) and others applied such models to predict the movement of monsoon depressions with encouraging results. The present work is to study the behaviour of two quasi-geostrophic models, *viz.*, a single level barotropic model at 500 mb and a two level baroclinic model applied at 250 mb and 750 mb, with wind as the basic input. It is now well recognised that wind measurements over the tropics are generally far more reliable than the observed geopotential height values, particularly over the southern parts of the Indian Peninsula, where the spatial gradients of geopotential heights are rather weak. The wind fields in these latitudes (below 15 deg. N), therefore provide a better representation of synoptic patterns. The models are applied to two synoptic situations with depression in the Bay of Bengal and one with depression in the Arabian Sea during summer Monex-79. Mean values of the diagnostic parameters, such as the vorticity, the square of absolute vorticity and the total kinetic energy etc, are monitored during the course of integration so as to examine the invariance of these quantities in the two models. The relative performance of the two models and the forecast errors are also discussed.

2. Model equations

The formulations of the two models are given in detail in this section. Symbols used are :

θ : latitude

p : pressure

z : height in metres

$\triangle y$: grid distance in the north-south (y) direction

$\triangle x$: grid distance in the east-west (x) direction $= \triangle y \cos \theta$

$\triangle p$: pressure-interval between levels 0-2 and 2-4 = —500 mb

$\triangle t$: time interval = 1 hour

V : horizontal wind vector

u, v : components of V in the x and y directions respectively

ω : vertical velocity $= dp/dt$

g : acceleration due to gravity $= 9.8$ metres/sec^2

R : radius of the earth = 6371.229 km

Ω : angular velocity of the earth $= 7.29 \times 10^{-5}$/sec

f : Coriolis parameter $= 2\ \Omega \sin \theta$

$\beta : \dfrac{\partial f}{\partial y} = \dfrac{2\Omega \cos\theta}{R}$

ψ : stream function, defined by $\mathbf{V} = \mathbf{k} \times \nabla\psi$, where $\mathbf{k}$ is the vertical unit vector and ∇ is the horizontal Nabla operator

ξ : relative vorticity $= \nabla^2\psi$

η : absolute vorticity $= \xi + f$

ϕ : geopotential height $= gz$

T : temperature

θ_T : potential temperature

σ : static stability parameter $= \dfrac{\partial \phi}{\partial p} \cdot \dfrac{\partial \log \theta_T}{\partial p}$

∇^2 : Laplacian operator $= \left(\dfrac{\partial^2}{\partial x^2} + \dfrac{\partial^2}{\partial y^2} \right)$

$J(a, b)$: Jacobian operator $= \left(\dfrac{\partial a}{\partial x} \cdot \dfrac{\partial b}{\partial y} - \dfrac{\partial a}{\partial y} \cdot \dfrac{\partial b}{\partial x} \right)$

c_p : specific heat at constant pressure.

Model I : Non-divergent quasi-geostrophic barotropic model

One-level non-divergent quasi-geostrophic model is based on the simplified vorticity equation :

$$\frac{\partial}{\partial t} (\nabla^2\psi) = -J(\psi, \eta) \qquad (1)$$

Model II : Two level quasi-geostrophic baroclinic model

This model is based on the vorticity equation in the form :

$$\frac{\partial}{\partial t} (\nabla^2\psi) = -J(\psi, \eta) + \eta \frac{\partial \omega}{\partial p} \qquad (2)$$

applied at the two levels, *i.e.*, 250 mb and 750 mb of the atmosphere and the omega equation :

$$\sigma \nabla^2\omega + f^2 \frac{\partial^2 \omega}{\partial p^2} = f \frac{\partial}{\partial p} J(\psi, \eta) - \nabla^2 J\left(\psi, \frac{\partial \phi}{\partial p} \right) \qquad (3)$$

applied at the intermediate level of 500 mb.

While the single level used in the barotropic model is assumed to represent the whole atmosphere, the two levels in the baroclinic model are assumed to represent conditions respectively in the upper and lower layers of the atmosphere. The vertical resolution of the baroclinic model and the parameters assigned at different levels are as follow :

Pressure (mb)	*Model parameters*	*Level*
0	$\omega_0 = 0$	0
250	ψ_1, η_1, ϕ_1	1
500	ω_2	2
750	ψ_3, η_3, ϕ_3	3
1000	$\omega_4 = 0$	4

Eqn. (2) is applied at levels 1 and 3, while Eqn. (3) is applied at level 2. The vertical boundary conditions for Eqn. (3) are $\omega = 0$ at the top and bottom of the atmosphere. With these boundary conditions, the vorticity Eqn. (2) for the two levels become :

Level 1 :

$$\frac{\partial}{\partial t} (\nabla^2\psi_1) = -J(\psi_1, \eta_1) - \eta_1 \frac{\omega_2}{\Delta p} \qquad (4)$$

Level 3 :

$$\frac{\partial}{\partial t} (\nabla^2\psi_3) = -J(\psi_3, \eta_3) + \eta_3 \frac{\omega_2}{\Delta p} \qquad (5)$$

and the omega Eqn. (3) reduces to :

$$\sigma \nabla^2\omega_2 - 2f^2 \omega_2/(\Delta p)^2 = f \frac{J(\psi_1, \eta_1) - J(\psi_3, \eta_3)}{\Delta p} - \nabla^2 J\left(\frac{\psi_1 + \psi_3}{2}, \frac{\phi_1 - \phi_3}{\Delta p} \right) \qquad (6)$$

3. Computational procedure

A five-point finite difference approximation for the Jacobian operator $J_{i,j}(a, b)$ and the Laplacian operator $\nabla^2_{i,j}(a)$ at grid point (i, j) is used as follows :

$$J_{i,j}(a, b) = [(a_{i+1,j} - a_{i-1,j})(b_{i,j+1} - b_{i,j-1}) - (a_{i,j+1} - a_{i,j-1})(b_{i+1,j} - b_{i-1,j})] / 4\Delta x \Delta y$$

$$\nabla^2_{i,j}(a) = \frac{a_{i+1,j} + a_{i-1,j} - 2a_{i,j}}{(\Delta x)^2} + \frac{a_{i,j+1} + a_{i,j-1} - 2a_{i,j}}{(\Delta y)^2}$$

The relative vorticity field for both models is obtained from the observed wind field by using the relation :

$$\zeta = \frac{\partial v}{\partial x} - \frac{\partial u}{\partial y} \qquad (7)$$

With zero lateral boundary conditions, the Poisson type equation $\nabla^2\psi = \zeta$ is then solved by Liebmann's successive relaxation scheme to obtain a stream function field ψ. An over-relaxation factor of 1.4 is used for quick convergence of the relaxation process. The stream function and the absolute vorticity η fields so obtained form the initial input to the model I. In the case of model II, the non-linear balance equation :

$$\nabla^2\phi = f\nabla^2\psi + \beta \frac{\partial \psi}{\partial y} + 2J\left(\frac{\partial \psi}{\partial x}, \frac{\partial \psi}{\partial y} \right) \qquad (8)$$

is solved with observed values of geopotential heights at lateral boundary as the boundary condition to obtain balanced geopotential height fields at levels 1 and 3. Saha and Suryanarayana (1971) found that this type of balance relation described mutually consistent flow patterns in wind and geopotential

fields. Using the values of ψ, $\nabla^2\psi$ and ϕ so determined at levels 1 and 3, the omega Eqn. (6) is solved by a relaxation technique assuming zero lateral boundary conditions and a constant value for static stability σ. The vorticity tendencies $\partial/\partial t\ (\nabla^2\psi)$ at levels 1 and 3 are then obtained from Eqns. (4) and (5) .

4. Time integration scheme

A time-differencing scheme with the first time step forward and the subsequent time steps centered is used for integration of both the models. The sequence of operations leading to the final forecast may be itemised as follows :

4.1. *Model I*

(*a*) From given wind field, the vorticity $\nabla^2\psi$ and stream functon ψ are first calculated.

(*b*) The vorticity tendency $[(\partial/\partial t)(\nabla^2\psi)]$ is then calculated using Eqn. (1).

(*c*) The vorticity $\nabla^2\psi$ at the first time step is calculated using the relation :

$$(\nabla^2\psi)_{t+\Delta t} = (\nabla^2\psi)_t + \Delta t \left(\frac{\partial}{\partial t}\nabla^2\psi\right)_t \quad (9)$$

(*d*) The vorticity at subsequent time steps, *i.e.*, second and onward, is calculated using the relation:

$$(\nabla^2\psi)_{t+\Delta t} = (\nabla^2\psi)_{t+(n-2)\,\Delta t} + 2\,\Delta t \left(\frac{\partial}{\partial t}\nabla^2\psi\right)_{t+(n-1)\,\Delta t} \quad (10)$$

where, in the subscripts, '*n*' denotes the number of time steps and takes integral values equal to, or greater than, 2.

Steps (*a*) to (*d*) are repeated to cover the entire period of integration which is of 24 hours duration in the present case. A predicted vorticity and stream function field is thus obtained.

4·2. *Model II*

(*a*) From given wind field, the vorticity $\nabla^2\psi$ and stream function ψ fields are first calculated at levels 1 and 3.

(*b*) With the observed geopotential height values at the lateral boundaries the entire balanced geopotential height field ϕ is obtained by solving the non-linear balance Eqn. (8) at both levels 1 and 3.

(*c*) The omega Eqn. (6) is then solved at level 2 to obtain ω_2.

(*d*) The tendency $[(\partial/\partial t)(\nabla^2\psi)]$ is then calculated at levels 1 and 3 by using Eqns. (4) and (5) respectively.

(*e*) The vorticity at the first and subsequent time steps is then calculated following the time integration scheme given by Eqns. (9) and (10) respectively.

With these new values of $\nabla^2\psi$, steps (*a*) to (*e*) are repeated to obtain a 24-hour forecast. Finally, a predicted vorticity and stream function field is obtained at levels 1 and 3 and a predicted vertical velocity field is obtained at level 2.

To avoid separation of solutions of alternate time steps arising out of computational mode of centred finite time differencing scheme, a mild Robert time filter (Robert, 1966) is used in both the models during integration. This filter may be written as :

$$A^*_{t-1} = A_{t-1} + 0.05\,(A^*_{t-2} - 2\,A_{t-1} + A_t)$$

where A^* is the filtered value of A and subscripts t, $t-1$, $t-2$ indicate time levels.

To examine the energy conserving properties of the two models, area averages of the following elements were monitored :

Model I — Kinetic energy (KE), absolute vorticity (TE) and square of absolute vorticity (TE²).

Model II — Kinetic energy (KE), available potential energy (APE), their sum, *i.e.*, (KE+APE) and the total energy (TE), *i.e.*, the sum of potential energy, gz, internal energy, c_pT, and the kinetic energy, KE; $(gz+c_pT+\mathrm{KE})$.

5. Model domain, grid and data used

Both the models are applied to an area extending from 5° N to 35° N latitudes and from 60° E to 100° E longitudes with a 2.5° Lat. Long. grid for computation of horizontal differencing. Input to both the models are manually analysed streamline-isotach fields at relevant isobaric surfaces. In model II, the pressure interval Δp is taken as — 500 mb and a constant value of 0.041 m² /sec² / mb² is assumed for the static stability parameter σ.

The synoptic situations to which the models are applied have each a monsoon depression in the field, centred at 12 GMT of date as follows :

Date	*Position of centre of depression*
17 June 1979	15.0 °N, 67.0 °E
6 July 1979	18.0 °N, 86.5 °E
13 August 1979	19.5 °N, 91.0 °E

6. Results

Predicted wind and stream function patterns are compared to the observed non-divergent wind and stream function fields of the following day. Results of this comparison may be summarised as follows :

6·1. *Model I*

Figs. 1, 2 and 3 show the results of forecast with model I in the case of the synoptic situation at initial maptime 12 GMT, 13 August 1979. As seen from Fig. 1, the centre of depression lies at 19.5° N, 91.0° E. Another low pressure area lies over the western part of the country centred at 24.0° N, 69.5° E. A broad anticyclonic circulation is seen to lie over the northern part of

the domain. From the forecast field in Fig. 2, it is noticed that the Bay depression has moved to 20.0° N, 87.0° E, while the other low has remained nearly stationary over the western part of the country. The anticyclonic circulation has become diffused to a large extent. Finally from Fig. 3, which gives the observed field at 12 GMT of 14 August 1979, the actual position of the Bay depression is now at 21.5° N, 87.0° E which indicates movement in a more northerly direction than the forecast movement. The other low has become unimportant and now lies as a week cyclonic circulation centred at 23.0° N, 64.0° E. Another weak cyclonic circulation has formed over the central part of the country which has not been predicted by the model.

The variation of average kinetic energy (KE), absolute vorticity (TE) and square of absolute vorticity (TE^2) as the percentage of their initial values, during the course of integration is shown in Fig. 9(a). We notice that the absolute vorticity and square of absolute vorticity have varied during the 24-hour integration within 1 per cent of their initial value. The kinetic energy change is however about 6 per cent. This is equivalent to change in wind speed less than 3 per cent. An examination of u and v variation separately, showed that a larger part of this change is contributed by the change in zonal kinetic energy. Considering other cases also, it was observed that kinetic energy and vorticity were not strictly conserved, although the conservation of vorticity was better than that for kinetic energy. This may be due to the boundary conditions used, in which the vorticity values at the boundaries are changed at every time step while extrapolating them for calculating the Jacobian terms in the model equations. This procedure does not strictly conserve vorticity and kinetic energy.

6.2. *Model II*

The 250 mb charts have not been shown here as the main focus of attention in this paper is the movement of the centre of depressions which do not extend to this level. From Fig.4, which gives the initial position of depression it may be seen that the centre of depression over the Bay of Bengal lies at 750 mb at 22.0° N, 92.0° E at 12 GMT, 13 August 1979. The other low pressure over the western part of the country is centred at 24.5° N and 73.0° E. Fig. 5 shows slight weakening of the Bay depression in 24 hours forecast, as seen from the stream function values, and is now centred at 22.5° N, 91° E. The low over the western part of the country remained stationary and has somewhat intensified. A week anti-cyclonic circulation developed over the southwestern part of the domain. From Fig. 6, we see that the actual position of the centre of the depression at this level over the Bay is at 22.0° N, 91.0° E, indicating an actual movement in a more southerly direction than the predicted movement. Contrary to forecast results the depression also intensified. The intensification of other low

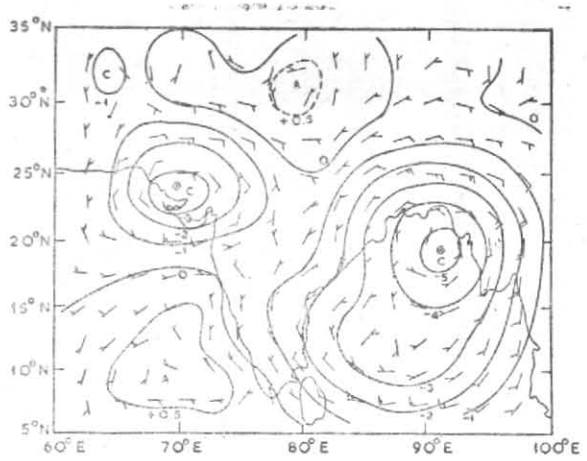

Fig. 1. Observed stream function and wind fields at 500 mb at 12 GMT, 13 August 1979. C—Cyclonic; A—Anticyclonic (solid lines indicate stream function values in units 10^5 m^2 sec^{-1})

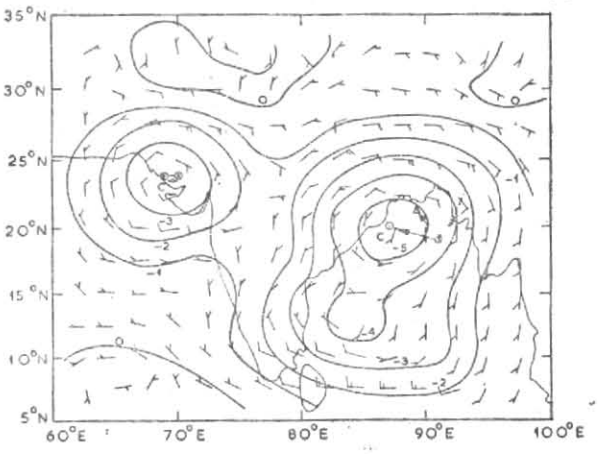

Fig. 2. Predicted 24-hour barotropic forecast fields of stream function and non-divergent wind at 500 mb at 12 GMT valid for 14 August 1979

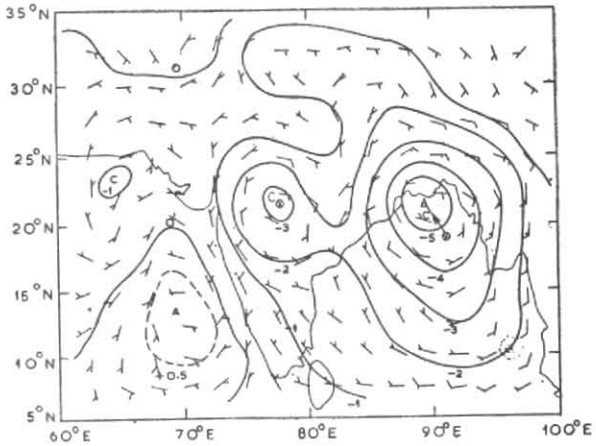

Fig. 3. Observed stream function and non-divergent wind fields at 500 mb at 12 GMT, 14 August 1979

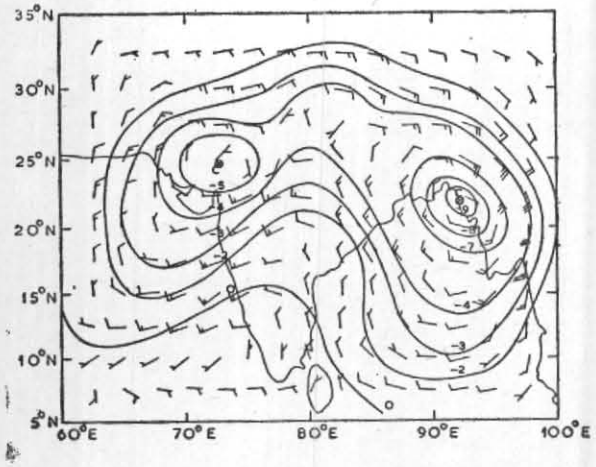

Fig. 4. As in Fig. 1 except at 750 mb

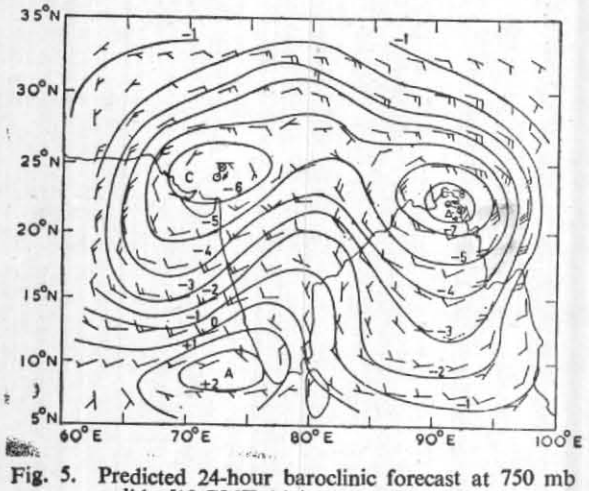

Fig. 5. Predicted 24-hour baroclinic forecast at 750 mb valid at 12 GMT, 14 August 1979.

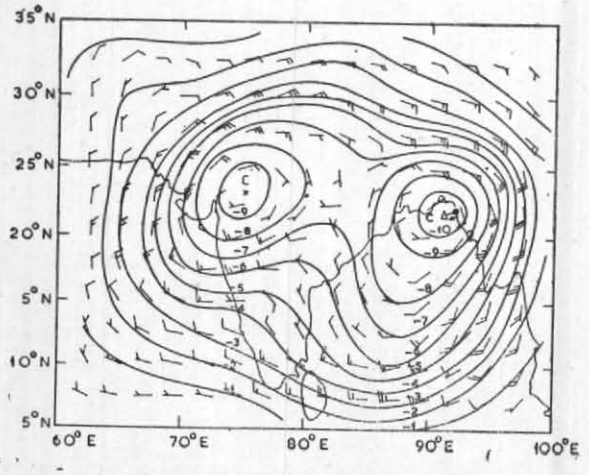

Fig. 6. As in Fig. 3 except at 700 mb

was also more than predicted. This system moved in a somewhat easterly direction. A comparison of the position of centres of both the Bay depression and the low over the western part of the country at 500 mb (Fig. 1) and 750 mb (Fig. 4) levels, show a southwestward tilt of the axis of these low pressure centres which confirms to an important features of monsoon depressions. In Fig. 7 and Fig. 8, the arrows pointing upwards indicate negative vertical velocity values (ω) or rising motion of air, while those pointing downwards indicate sinking motion of air. From these, we notice that the upward vertical velocity field did not show much change during the forecast period over the Bay of Bengal. Over the northern and western parts of the country, there is downward motion of air to the south, and weak upward motion to the north. Some weakening of the omega-field took place in the 24-hour prediction in this region. The reason for the existence of downward vertical velocity over this region, which is occupied by a cyclonic system at 750 mb, is hard to find. However, poor vertical resolution of the model and lack or upper air data over this region may have contributed towards this anomaly.

Fig. 9 (b) shows the variation of average kinetic energy (KE), available potential energy (APE) and the sum of kinetic and available potential energies (KE+APE). The variation of total energy (TE), *viz.*, the sum of the potential energy, gz, internal energy, c_pT and kinetic energy, KE is shown in Fig. 9(c). It may be seen that the kinetic energy increased slightly (maximum increase is of about 0.7 per cent) during the first half of integration, and then decreased to nearly its initial value during the second half of the integration period. Available potential energy has increased by about 5.5 per cent in 24 hours and the sum (KE+APE) increased by 3 per cent. The change in the total energy (TE), however, is found to be negligible (an increase of about 0.01 per cent). Thus the model satisfies its energy conserving properties fairly well. The increase is APE by 6 per cent in 24 hours may be due to the unsatisfactory boundary conditions, as already explained in section 6.1.

6.3. *Comparative performance of the two models*

A comparison of integration of both the models, for the three synoptic situations studied, is shown in Figs. 10 (a) and 10 (b). The depression in the central Arabian Sea on 17 June 1979 showed a southsouthwesterly movement at 500 mb in model I, while the actual movement was in a more northnorthwesterly direction. In model II, the same depression at 750 mb moved in a westerly direction, while the predicted movement was in a westsouthwesterly direction, showing a better agreement between actual and forecast movement

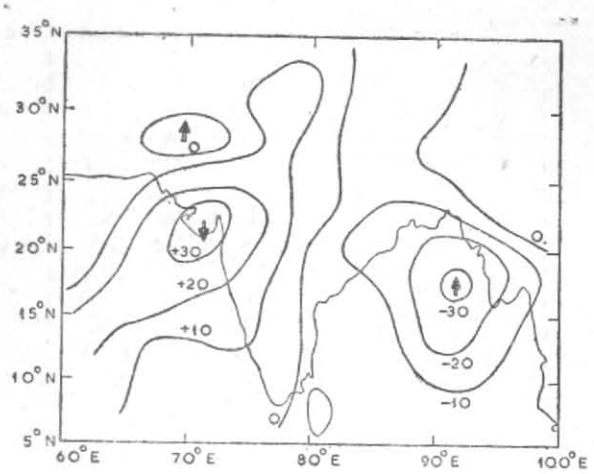

Fig. 7. Initial omega ($\omega \times 10^{-5}$ mb sec $^{-1}$) field at 500 mb at 12 GMT, 13 August 1979

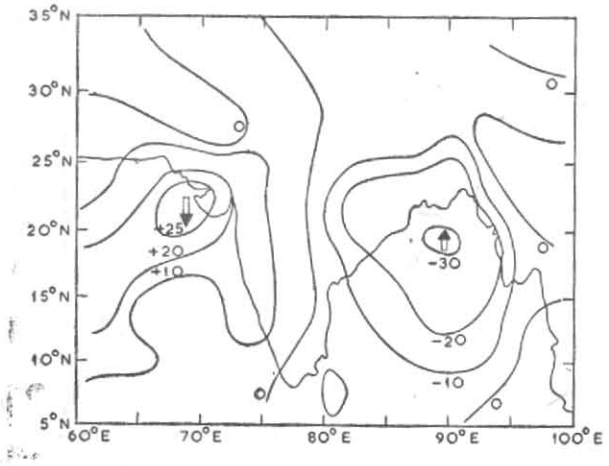

Fig. 8. 24-hour baroclinic forecast omega field at 500 mb at 12 GMT valid for 14 August 1979

than in model I. The predicted movement of the Bay of Bengal depression of 6 July 1979 in both the models was unrealistic as compared to its actual movement. However, the result of model II, in this case, is also better than of model I. The performance of model II for the 13 August 1979 depression in the Bay of Bengal is also seen to be better than model I.

It may be noted, that except for the depression of 6 July 1979, the prediction of the westerly component of the depressions agrees well with their actual movement in this direction. Thus the errors in the forecasts can mainly be attributed to errors in predicting their meridional movements.

7. Conclusion

From above, we notice that a single-level barotropic model and a two-level baroclinic model is able to predict the movement of monsoon depressions to some degree accuracy. The performance of the two level model has been found to be decisively better than that for the one-level model. A higher vertical resolution is likely to further improve the performance of the quasi-geostrophic baroclinic model. Monsoon depressions are characterised by their westward movements which have been well predicted by both the models. However, the meridional component of the depression movements, though small, are found to be in error during model prediction. The errors in the vertical velocity

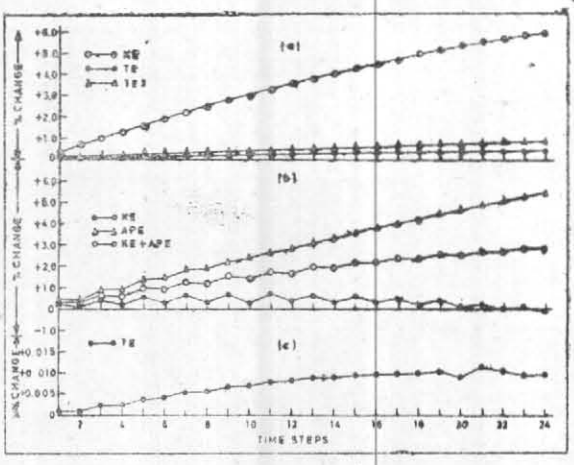

Fig. 9. Percentage change with time step in the average values of :

(a) kinetic energy (KE), absolute vorticity (TE) and square of absolute vorticity (TE^2), for model I

(b) kinetic energy (KE), available potential energy (APE) and their sum, *i.e.*, (KE+APE), for model II

(c) total energy (TE), *i.e.*, the sum of the potential energy, gz, internal energy, c_pT and kinetic energy, KE; ($gz+c_pT$+KE), for model II

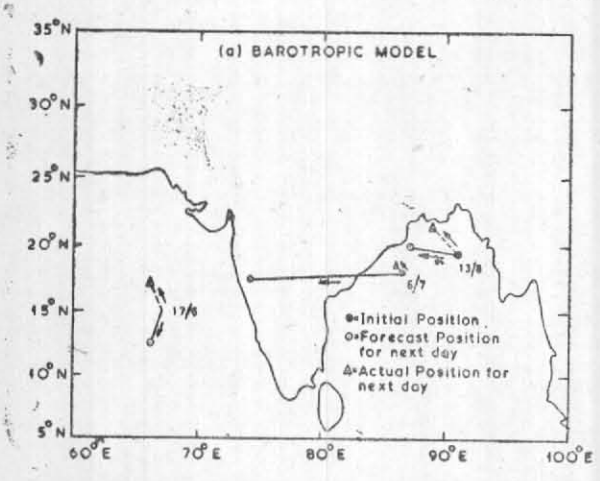

Fig. 10 (a). Comparison of 24-hour forecast with observed position of the centre of depression for the three synoptic situations studied : (a) model I (barotropic)

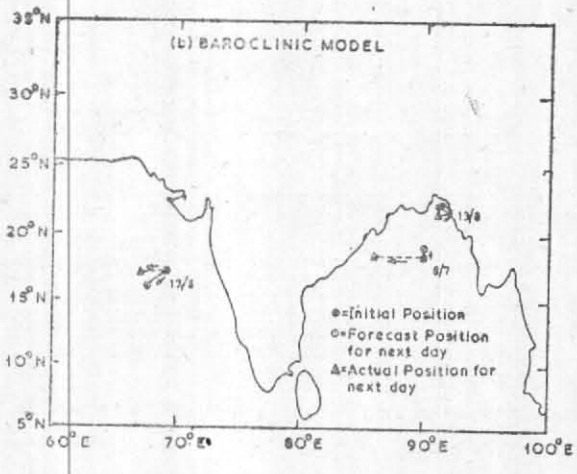

Fig. 10 (b). Model II (baroclinic), date/month of the depression are indicated near its initial position

field obtained during integration of model II were more in the case of depressions over the Arabian Sea than over the Bay of Bengal. Poor vertical resolution of the model may be one of the reasons for this error in prediction and requires closer examination

Acknowledgements

Thanks are due to Dr. G. P. Malik, School of Environmental Sciences, Jawaharlal Nehru University, New Delhi, for this encouragement throughout this study and to Dr. P. K. Das, Director General of Meteorology, India Meteorological Department, for making available important Monex-79 data on which this research work is based. The author also acknowledges the guidance and useful suggestions provided by Dr. K. R. Saha and Dr. H. S. Bedi during the course of this work. The research reported in this paper forms part of the work to be submitted by the author to the Jawaharlal Nehru University for the award of the degree of Doctor of Philosophy.

References

Mukherji, T. K. and Datta, R. K., 1973, Prognosis by four layer quasi-geostrophic model, *Indian J. Met. Geophys.*, **24**, pp. 93-100.

Robert, A. J., 1966, The integration of low order spectral form of the primitive meteorological equations, *J. met. Soc. Japan*, Sr. II, **44**, 5, pp. 237-245.

Saha, K. R. and Suryanarayana, R., 1971, Numerical solutions of geopotential with different forms of balance relationships in the tropics, *J. met. Soc. Japan*, Sr. II, **49**, pp. 510-515.

Shukla, J. and Saha, K. R., 1970, Applications of non-divergent barotropic model to predict flow patterns in the Indian region, *J. met. Soc. Japan*, **48**, pp. 405-409.